Environmental Science & Technology

Article

Cite This: Environ. Sci. Technol. 2019, 53, 5758−5767

pubs.acs.org/est

Organic Functional Group Chemistry in Mineralized Deposits Containing U(IV) and U(VI) from the Jackpile Mine in New Mexico

Carmen A. Velasco,[†] Kateryna Artyushkova,[‡] Abdul-Mehdi S. Ali,[§] Christopher L. Osburn,[∥] Jorge Gonzalez-Estrella,[†] Juan S. Lezama-Pacheco,[⊥] Stephen E. Cabaniss,[#] and José M. Cerrato*[,†]

[†]Department of Civil, Construction & Environmental Engineering, MSC01 1070, University of New Mexico, Albuquerque, New Mexico 87131, United States

[‡]Department of Chemical and Biological Engineering, MSC01 1120, University of New Mexico, Albuquerque, New Mexico 87131, United States

[§]Department of Earth and Planetary Sciences, MSC03 2040, University of New Mexico, Albuquerque, New Mexico 87131, United States

[∥]Department of Marine, Earth, and Atmospheric Sciences, North Carolina State University, Raleigh, North Carolina 27607, United States

[⊥]Department of Environmental Earth System Science, Stanford University, Stanford, California 94305, United States

[#]Department of Chemistry and Chemical Biology, University of New Mexico, Albuquerque, New Mexico 87131, United States

Supporting Information

ABSTRACT: We investigated the functional group chemistry of natural organic matter (NOM) associated with both U(IV) and U(VI) in solids from mineralized deposits exposed to oxidizing conditions from the Jackpile Mine, Laguna Pueblo, NM. The uranium (U) content in unreacted samples was 0.44−2.6% by weight determined by X-ray fluorescence. In spite of prolonged exposure to ambient oxidizing conditions, ≈49% of U(IV) and ≈51% of U(VI) were identified on U L_{III} edge extended X-ray absorption fine structure spectra. Loss on ignition and thermogravimetric analyses identified from 13% to 44% of NOM in the samples. Carbonyl, phenolic, and carboxylic functional groups in the unreacted samples were identified by fitting of high-resolution X-ray photoelectron spectroscopy (XPS) C 1s and O 1s spectra. Peaks corresponding to phenolic and carbonyl functional groups had intensities higher than those corresponding to carboxylic groups in samples from the supernatant from batch extractions conducted at pH 13, 7, and 2. U(IV) and U(VI) species were detected in the supernatant after batch extractions conducted under oxidizing conditions by fitting of high-resolution XPS U 4f spectra. The outcomes from this study highlight the importance of the influence of pH on the organic functional group chemistry and U speciation in mineralized deposits.

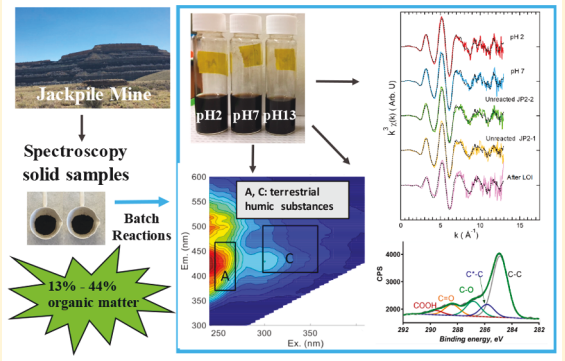

INTRODUCTION

The legacy of operations for uranium (U) mining in the United States has impacted several sites, many of which are located in Native American communities. Studies have reported U concentrations of 35.3−772 $\mu g\ L^{-1}$ in surface waters near the Pueblo of Laguna, New Mexico (NM), neighboring the Jackpile Mine.[1] These concentrations exceed the U.S. Environmental Protection Agency (EPA) maximum contaminant level of 30 $\mu g\ L^{-1}$.[2] Additionally, the U concentration detected in solid samples from the Jackpile Mine, adjacent to the Rio Paguate, was 9300 mg kg^{-1}.[1] A recent study in the Grants Mining District in NM reports that the mineralogy of U-bearing dust affects the extent of U dissolution in simulated lung fluids, which could have potential health implications.[3] The Jackpile Mine has been listed in the EPA National Priorities List for CERCLA cleanup.[4]

Natural organic matter (NOM) and U co-occur in the Jackpile Sandstone Member of the Morrison Formation. Sandstone formations are characterized by varied sizes of sorted pebbles and sands and lenses of concentrated NOM.[5] Uranium is trapped within the NOM layers of detritus and humus, leading to the formations of deposits rich in NOM and U.[6] Reduced U was found in solid samples from mineralized deposits in the Jackpile Mine despite being exposed to oxidizing conditions for several decades.[1] Studies have found coffinite [$USiO_{4(s)}$] as crystals precipitated or embedded in layers of amorphous NOM-bearing grain coatings in the

Received: January 18, 2019
Revised: April 12, 2019
Accepted: April 18, 2019
Published: April 18, 2019

DOI: 10.1021/acs.est.9b00407
Environ. Sci. Technol. 2019, 53, 5758−5767

Grants region, NM.[7−11] Natural organic matter may enhance the preservation of U(IV) phases exposed to oxidizing fluids for more than 30 million years.[5,12]

Organic functional groups play a key role in the chemical speciation and reactivity of U and other metals in the environment. Dissolved humic substances facilitate the transport of U and other metals as a function of pH by affecting the sorption on mineral surfaces.[13−16] It has been reported that soluble U complexes with humic substances in peats.[17] The formation of U(VI)−humate complexes between pH 4 and 6 can influence sorption of U on NOM.[17,18] Previous studies found U is predominantly bound in bidentate−mononuclear complexes to carboxyl ligands in natural NOM, inhibiting the precipitation of U minerals.[19−22] Furthermore, U(IV) can complex with NOM functional groups, resulting in the formation of monomeric U(IV) species that have been observed in anoxic sediments and ore deposits together with other crystalline U(IV) phases such as uraninite.[23−26] Other studies reported NOM complexation influences the abiotic oxidation rate of Fe(II) by O_2.[27−29] For example, functional groups such as quinones act as terminal electron acceptors in anaerobic microbial respiration, while phenols serve as electron donors for the reduction of electron acceptors, such as Fe(III), Mn(IV), arsenate, Cr(VI), and U(VI).[30−32] Despite these findings, the influence of pH on the organic functional group chemistry and the speciation of U(IV) and U(VI) co-occurring in U mine sites remains unknown.

. While the presence of NOM in sandstone formations is well established, the organic functional group chemistry has not been extensively studied.[1,33−35] Improving the current understanding of the organic functional group chemistry found in sandstone formations and mineralized U deposits will help to identify the binding mechanisms influencing the interactions of U and NOM. These interactions may ultimately affect the reactive transport of . U in soils, surface water, groundwater, and uptake in plants.[36] Although several methods have been used to understand the mineralogy of sandstone formations and U mineralized deposits, the analysis of particulate NOM is challenging.[6] The application of X-ray photoelectron spectroscopy (XPS) to observe changes in organic functional groups in U mineralized deposits as a result of pH changes is not well documented.[37,38] Integrating XPS analyses with other physical and chemical methods could provide new information about NOM functional chemistry in U samples from mineralized deposits.

The objective of this study is to identify the organic functional group chemistry in U mineralized deposits from the Jackpile Mine. We integrated excitation−emission matrix spectroscopy (EEMS), XPS, X-ray absorption spectroscopy (XAS), thermal analyses, and batch extraction experiments. A novel aspect of this investigation is identifying the influence of pH on the organic functional group chemistry and the speciation of U(IV) and U(VI) co-occurring in samples of complex mineralogy from a sandstone geological formation through the integration of a variety of analytical techniques with laboratory experiments. The results of this study provide insights about the reactions between NOM and U in mineralized deposits that are relevant for risk assessment and remediation strategies.

MATERIALS AND METHODS

Sample Collection. Two solid samples (JP_1 and JP_2) from mineralized deposits from the Jackpile Mine (35°8′28.09″N, 107°20′19.67″W) were collected from a location described in a previous study.[1] Samples were collected in the summer of 2017, crushed, and sieved with a US Standard #230 mesh (63 μm). We referred to the crushed and sieved solids before any treatment was applied as "unreacted samples".

Solid Analyses. Solid phase analyses were conducted on unreacted samples by X-ray fluorescence (XRF) and C, H, N, and O elemental analysis. XAS and XPS were performed on unreacted samples, on reacted solids after loss on ignition (LOI), and on solids remaining from batch extraction experiments. XAS measurements were conducted at beamline 7-3 at the Stanford Synchrotron Radiation Laboratory (SSRL) at the U L_{III} edge in fluorescence mode. Data were collected at room temperature in a He-purged environmental chamber. Linear combination fitting was performed using the following reference materials as end members as measured from other studies: monomeric U(IV),[39] uraninite,[40] U(VI) adsorbed with ferrihydrite,[41] and the coffinite reference obtained from the Mineral Collection from the University of New Mexico. References and standards were pulverized and pressed into the slots of aluminum holders and sealed with Kapton tape on both sides. Data processing and analyses for XAS were conducted using Athena and Artemis.[42] A Kratos Ultra DLD X-ray photoelectron spectrometer was used to acquire the near surface (<10 nm) atomic composition and oxidation states. Survey spectra were acquired at 80 eV and high resolution at a 20 eV pass energy. A monochromatic Al source was used at a 150 W power to obtain C 1s and U 4f high-resolution spectra from the top ∼4−10 nm of the surface. Three areas per replicate were analyzed, and averages and standard deviations are reported. Shirley background subtraction was used to process the spectra using CasaXPS software.

Additional details about these methods are included in Supporting Information.

Acid Digestion and Solution Metal Analyses. Acid digestions were conducted in triplicate to assess the U acid-extractable content from the mineralized surface deposit solids, by adding 2 mL of HNO_3, 6 mL of HCl, and 3 mL of concentrated HF to 50 mL Teflon digestion tubes containing 2.000 ± 0.002 g of homogenized samples. Inductively coupled plasma optical emission spectroscopy (ICP-OES) and inductively coupled plasma mass spectrometry (ICP-MS) measured metal concentrations in solution. Additional details about these methods are included in Supporting Information.

Thermal Analyses for Solids. The NOM content in the mineralized deposit solid samples was estimated by LOI and thermogravimetric analyses (TGA). Details of these methods are provided in Supporting Information.

Extraction of Natural Organic Matter. Natural organic matter from the mineralized deposit solid samples was identified by a modified approach of the Nagoya method as described in a study conducted to characterize humic substances by EEMS and parallel factor analysis.[43,44] Detailed information about batch extractions is in Supporting Information. Briefly, NOM was extracted with a 0.1 N NaOH solution at pH 13. Reactions were carried out in triplicate for 24 h at 4 °C. A set of batch reactors was acidified from pH 13 to 7 with concentrated trace metal grade HCl. Exposing these samples to pH 7 is environmentally relevant because circumneutral pH conditions are characteristic of the Rio Paguate near the Jackpile Mine.[1] Another set of batch reactors was acidified from pH 13 to 2. Exposing these samples to pH 2 is relevant because acid drainage has been observed in

DOI: 10.1021/acs.est.9b00407
Environ. Sci. Technol. 2019, 53, 5758−5767

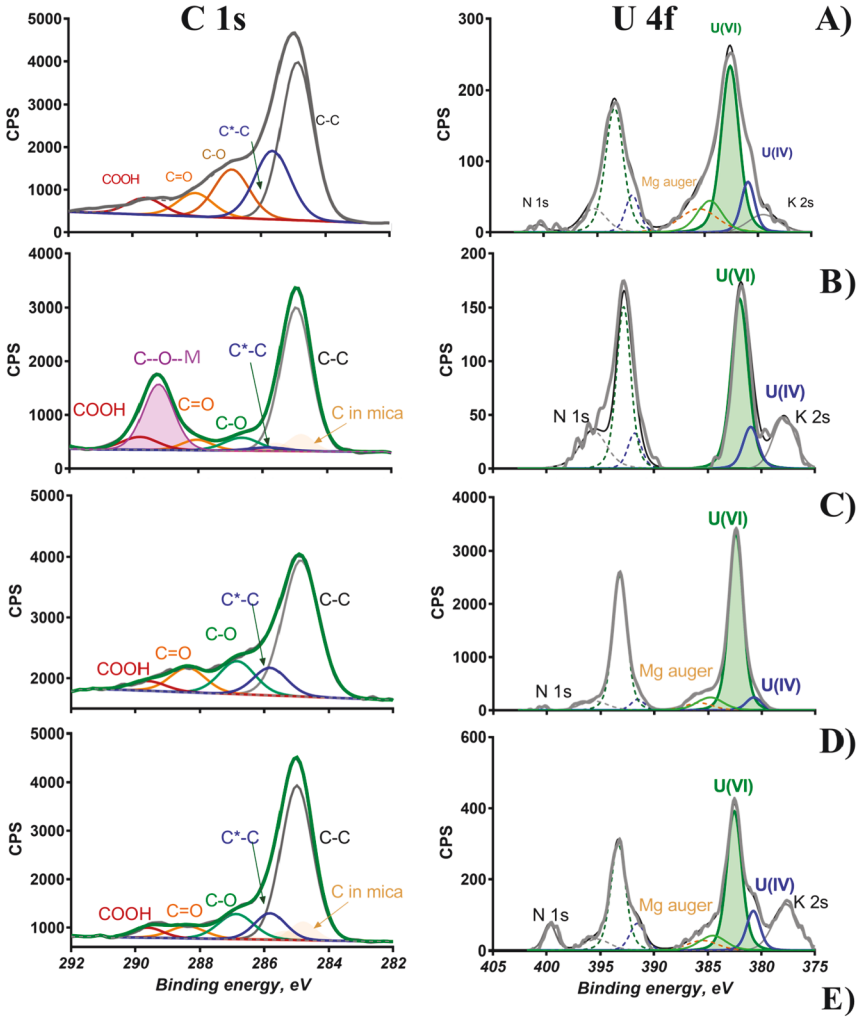

Sample	pH	Carbonyl (C=O)	Phenol (COH)	Carboxylic (COOH)	C-O-M	U (IV)	U (VI)
Unreacted Mine Wastes	as is	8.6%	18.3%	5.8%	0.0%	19.4%	80.6%
Supernatant	13	3.8%	5.4%	5.4%	23.5%	6.6%	93.4%
	7	10.7%	14.4%	4.2%	0.0%	22.1%	77.9%
	2	5.3%	11.0%	3.7%	0.0%	31.0%	69.0%
Reacted Solids	13	10.3%	14.6%	5.3%	0.0%	5.4%	94.6%
	7	5.7%	12.7%	3.6%	0.0%	15.0%	85.0%
	2	2.2%	5.9%	5.2%	0.0%	4.8%	95.2%

Figure 1. Fitting of high-resolution XPS carbon (C 1s) and uranium (U 4f) spectra of (A) unreacted Jackpile Mine solids. Fitting of high-resolution XPS carbon (C 1s) and uranium (U 4f) spectra of the supernatant from batch extraction reactors at (B) pH 13, (C) pH 7, and (D) pH 2. (E) Percent composition of C 1s and U 4f spectra.

mine waste sites.[45−47] Subsequently, after the pH was adjusted, samples were centrifuged, decanted, and filtered using a 0.2 μm filter. Supernatant samples were stored at 4 °C in the dark until EEMS analysis. Remaining solids (reacted solids) were stored for XAS and XPS analyses.

Excitation−Emission Matrix Spectroscopy (EEMS) Analyses. Excitation−emission matrix spectroscopy was used as a rapid, nondestructive, and sensitive method to provide information about the fluorescing fraction of the NOM. Absorbance spectra of dissolved NOM solutions were measured from 200 to 800 nm on a Varian Cary 300UV spectrophotometer in 1 cm quartz cells. Fluorescence spectra were acquired on a Varian Eclipse spectrofluorometer. Excitation wavelengths were sampled from 240 to 450 nm at 5 nm intervals; emission wavelengths were sampled every 2 nm from 300 to 600 nm. A Milli-Q water blank was subtracted from each absorbance and fluorescence measurement. Milli-Q water had an 18 MΩ resistivity and <5 ppb TOC. Samples were diluted if the absorbance in a 1 cm cell was greater than 0.4 at 240 nm. Corrections for fluorescence were made for lamp excitation intensity and detector emission responses, and afterward, corrections for inner filter effects were applied using standard approaches.[48] Finally, the results were calibrated first to the water Raman signal of each instrument and then in

DOI: 10.1021/acs.est.9b00407
Environ. Sci. Technol. 2019, 53, 5758−5767

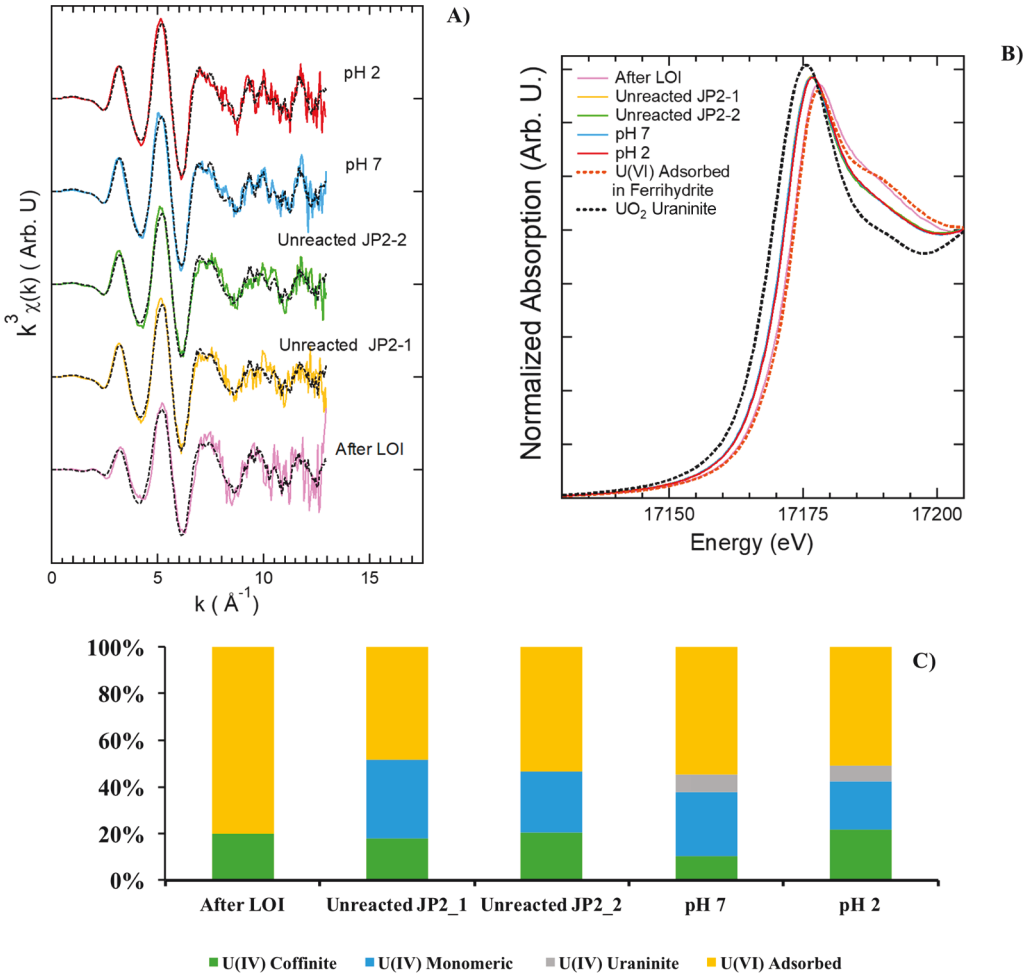

Figure 2. X-ray absorption spectroscopy (XAS) of unreacted and reacted solids (after LOI, pH 2 and 13) from the Jackpile Mine (JP_2). (A) U L_{III} edge EXAFS of the Jackpile Mine solid samples using the following references: uraninite, coffinite, and monomeric U(IV) for U(IV) and uranyl-adsorbed ferrihydrite as reference for U(VI). (B) Normalized bulk U L_{III} edge XANES spectra using uraninite (nano-UO_2) as a reference for U(IV) and adsorbed ferrihydrite as a reference for U(VI). (C) Linear combination fitting of the U L_{III} edge EXAFS spectra of U(VI) and U(IV) species in the Jackpile Mine solid samples.

quinine sulfate units (QSU). Fluorescence results were processed with an in-house MATLAB script (MathWorks, Natick, MA). Dissolved NOM was quantified by measuring the dissolved organic carbon (DOC) via automated heated-persulfate oxidation following an additional filtration through a 0.45 μm polyvinylidene fluoride filter.

Effect of pH on Organic Functional Chemistry and U Species. Batch extraction experiments assessed the effect of pH on the organic functional groups in the NOM from the mineralized deposit solids from the Jackpile Mine. For this set of reactions, we used the sample with the highest NOM content (JP_2) as determined by LOI and TGA. Natural organic matter was extracted by using 0.1 N NaOH, and after reaction for 24 h, the solution was acidified from pH 13 to 7 and from pH 13 to 2 with trace metal grade HCl. After the target pH had been reached, the supernatant was decanted and filtered through a 0.45 μm filter. Drops of the decanted and filtered supernatant at pH 13 (control), 7, and 2 were drop-cast on a freshly cleaved mica surface and allowed to dry. Dried supernatants and reacted solids from batch extraction experiments were then analyzed by XPS to obtain high-resolution spectra for C 1s, O 1s, and U 4f. The high-resolution C 1s and O 1s spectrum from freshly cleaved mica was obtained to account for the adventitious carbon present on the mica surface. Of the total carbon detected, <10% was due to adventitious carbon on the surface of freshly cleaved mica (Figure S1). The rest of the carbon corresponded to the NOM in the supernatant. Five peaks have been used to curve high-resolution C 1s spectra: aliphatic C−C at 285 eV, secondary carbon (C*−C−OH/C*−C═O) at 285.8 eV, phenol carbon at 286.5 eV, carbonyl carbon at 288.0 eV, and carboxylic C at 289.2 eV. Details about sample preparation for XPS analyses are provided in Supporting Information. Metal concentrations in the supernatant from each batch extraction reactor were analyzed by ICP-OES/ICP-MS. All reactions were carried out in triplicate.

RESULTS AND DISCUSSION

Uranium in Unreacted Mineralized Deposit Solid Samples from the Jackpile Mine. Samples contained 0.44 ± 0.03% (JP_1) and 2.61 ± 0.09% (JP_2) U by weight according to acid digestions and ICP-OES results. XRF analyses detected 1.02% (JP_1) and 8.22% (JP_2) U by weight. XRF and acid digestions are different approaches to measuring the concentration of U in the solid samples. XRF measures the total bulk concentration of a particular element, while acid

DOI: 10.1021/acs.est.9b00407
Environ. Sci. Technol. 2019, 53, 5758−5767

digestions determine the total acid-extractable elemental concentration. Both techniques quantify the elemental content in a a sample, and the results complement each other. The concentrations of U found in our samples are 3−4 orders of magnitude higher than the crustal U average of 2.78 mg kg^{-1}.[11] Previous studies have found co-occurrence of U and other elements in mine wastes and wetlands adjacent to the Jackpile Mine.[1,35]

Unreacted sample JP_2 showed 19.4 rel% U(IV) and 80.6 rel % U(VI) relative (rel) to the total U detected in the near surface by high-resolution U 4f XPS spectra (Figure 1A). Spectra from U L_{III} edge XANES on sample JP_2 also suggest that the unreacted solid samples contained a mixture of U(IV) and U(VI) (Figure 2). Unreacted samples averaged ≈49% U(IV) and ≈51% U(VI) according to the linear combination fitting of the U L_3 edge EXAFS spectra. Linear combination fits of the EXAFS spectra suggested samples contain more monomeric U(IV) (29%) than coffinite (19%) and also lack uraninite (Figure 2C and Table S1). Previous studies also found monomeric U, coffinite, and oxidized U in the Jackpile Mine as well as in an undisturbed U roll-front ore deposit in Wyoming, and in the microbial reduction of U(VI) in subsurface systems.[1,24,25,39] The proportions of U species found by XPS (near surface) and XAS (bulk) are different due to the characteristics of each technique. However, both results complement each other and confirm the existence of U(IV) and U(VI) in the surface and bulk part of our samples. Additional analyses were pursued to investigate the NOM physical and chemical characteristics from the Jackpile Mine.

Natural Organic Matter in Mineralized Deposits from the Jackpile Mine. *Natural Organic Matter Content.* LOI and TGA were used to estimate the NOM content in the unreacted samples (Figure 3). Sample JP_2 exhibited greater

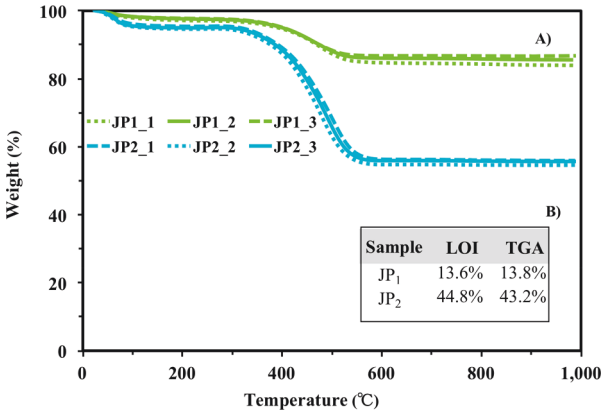

Figure 3. Thermal analyses [thermogravimetric analysis (TGA) and loss on ignition (LOI)] to estimate the organic matter content in solid samples from the Jackpile Mine mineralized deposits. (A) Change in mass content as a function of temperature (TGA) for unreacted solid samples JP_1 and JP_2. (B) Mass loss comparison between TGA and LOI.

mass loss (44.8 ± 0.22% by LOI and 43.19 ± 0.74% by TGA) than JP_1 (13.6 ± 0.26% by LOI and 13.84 ± 0.99% by TGA). Volatilization of NOM caused the mass loss in the samples. These results indicate that despite mining operations, NOM remained present in the Jackpile Mine. Other research found a lower content of NOM in the Jackpile Mine, ranging from 0.07% to 21.8% by LOI at 550 °C and from 1.2% to 2.8% by LOI at 850 °C, while wetlands adjacent to the Jackpile Mine contained 14−15% NOM by LOI.[1,33,35,49,50] A recent study in the Mulga Rock U deposit in Western Australia found that the LOI at 550 °C ranged from 1 to 57% by weight.[51] U L_{III} edge XANES analyses detected the oxidation of U in the solid samples after LOI (Figure 2B). The heat treatment (550 °C) likely oxidized the amorphous U(IV), while coffinite remained stable at this temperature. Other literature has also reported U oxidation when solids are exposed to high temperatures.[52]

Elemental Analysis. For this analysis, we used the sample with the highest NOM content (JP_2) as determined by LOI and TGA. Unreacted samples showed 33.2% C, 10.8% O, 1.4% H, and 0.16% N by weight for sample JP_2. These findings are within range of those of another study in the Grants Belt.[49] The low H/C ratio (0.513) indicates high aromaticity as suggested in other studies.[53,54] Moreover, low O/C (0.243) and (O + N)/C (0.247) ratios indicate low hydrophilicity and polarity.[53−56] Elemental analyses require a pure organic sample to avoid accounting for the C, O, H, and N from the minerals contained in the sample. The C detected with this technique is within the range identified by TGA and LOI.

Fluorescence Properties of Extracted Organic Matter from Mineralized Deposits from the Jackpile Mine. Excitation−emission matrix spectroscopy (EEMS) was used to assess the chemical properties of the fluorescing fraction of the NOM from the mineralized deposit samples from the Jackpile Mine. Samples JP_1 and JP_2 showed two major peak regions corresponding to the macromolecular signature of humic substances (Figure 4). Peak A corresponds to the excitation and emission wavelengths of 260 and 380−460 nm, respectively, and peak C corresponds to excitation and emission wavelengths of 320−360 and 420−460 nm, respectively, according to previous studies.[44,57] The change observed via EEMS at pH 2 is attributed to the precipitation of humic acids that are insoluble at low pH.[15,58] The dissolved organic carbon measured at pH 7 was 14.0 ± 1.7 mg L^{-1} for JP_1 and 8.7 ± 0.9 mg L^{-1} for JP_2.

Organic Functional Group Chemistry from Mineralized Deposits from the Jackpile Mine. Phenolic (18.3 ± 2.5 rel%) and carbonyl (8.6 ± 0.7 rel%) functional groups were more abundant, while carboxylic groups (5.8 ± 0.2 rel%) were the least abundant relative to the total carbon detected by high-resolution XPS C 1s and O 1s on the surface of unreacted solid samples (Figure 1 and Figure S2). Fitting of high-resolution XPS C 1s data showed the characteristic peaks for phenolic (286.5 eV), carbonyl (288 eV), and carboxylic (289 eV) functional groups in the unreacted solid samples. The peak due to secondary carbon (all carbons bound to phenolic, carbonyl, and carboxylic carbon) was included in the fit at 285.6 eV. Contrary to what has been reported in previous studies about NOM, we found that carboxylic functional groups were less abundant than phenols or carbonyls.[59,60] This finding is likely due to the fact that our samples are highly aromatic as indicated by the low H/C ratio. As suggested in other studies, the concentration of phenolic and carbonyl functional groups may affect the occurrence of U(IV) and U(VI), as both functional groups can influence the speciation of U found in our site.[31,59] Batch extraction experiments at pH 13, 7, and 2 were conducted to investigate changes in the functional chemistry of the NOM and U oxidation state as a function of solution pH.

Effect of pH on Organic Functional Group Chemistry. Fitting of high-resolution XPS C 1s and O 1s spectra shows more changes in peak intensity corresponding to phenolic and

DOI: 10.1021/acs.est.9b00407
Environ. Sci. Technol. 2019, 53, 5758−5767

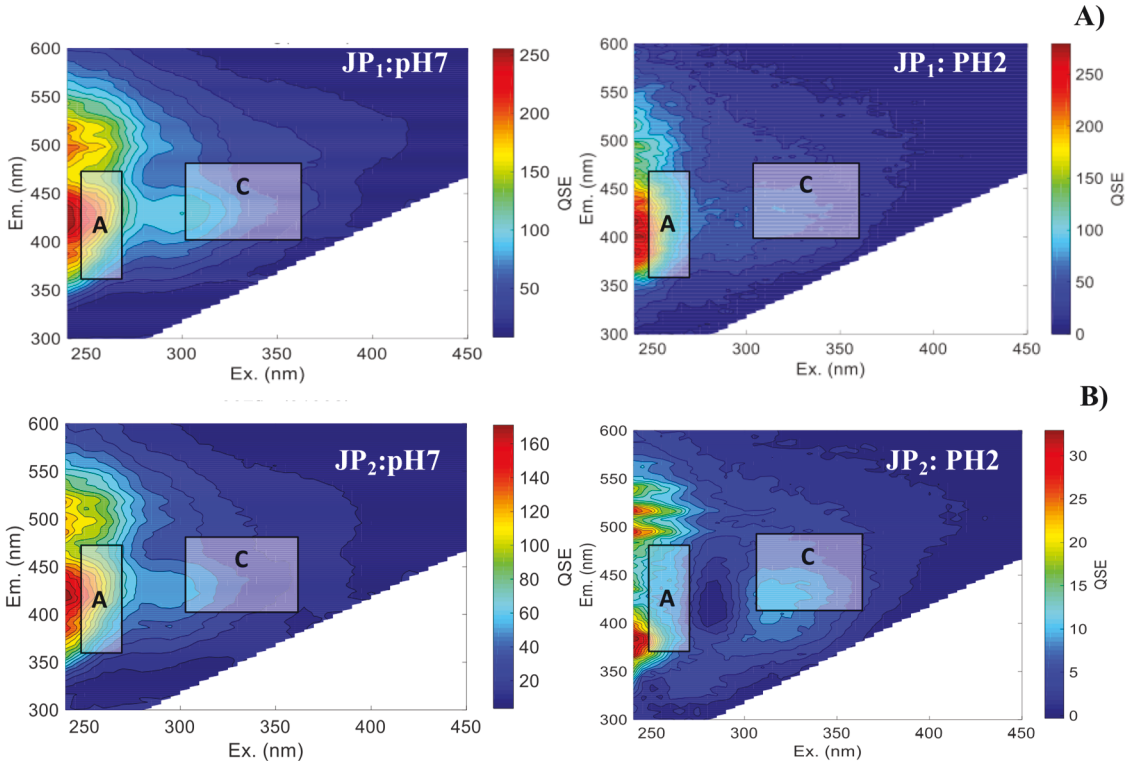

Figure 4. Results of excitation−emission matrix spectroscopy (EEMS) of the supernatant of batch extraction reactors at pH 7 and 2 from the Jackpile Mine samples: (A) JP_1 and (B) JP_2. Note the QSE scaling differences on the color bar for each EEM.

carbonyl functional groups compared to carboxylic groups in the supernatant in response to pH changes from batch extractions (Figure 1 and Figure S2). For instance, the relative percent of phenolic groups in high-resolution C 1s spectra increased with pH from 5.4 rel% at pH 13 to 14.4 rel% at pH 7 and to 11.0 rel% at pH 2. Likewise, the supernatant of the reactor at pH 13 contained 1.5−6.9 rel% fewer carbonyl groups than reactors at pH 7 and 2. In contrast to those of phenolic and carbonyl groups, the intensity of peaks corresponding to carboxylic groups in the supernatant of the reactor at pH 13 was similar to that of reactor supernatants at pH 7 and 2 (within a range of 1.2−1.7 rel%). Previous studies suggest that U in peat systems was coordinated to C atoms with carboxyl groups from particulate NOM through bidentate−mononuclear U(IV/VI) complexes.[26] Other studies found that U−phenolic bonds are prevalent at pH 6 while UO_2−carboxyl bonding is predominant at pH 3.5.[61] Furthermore, research found that U(VI) was immobilized by natural NOM and reduced U(IV) was bound with carboxylic groups in plant roots.[62]

Our XPS data indicate a possible complexation at pH 13 between carboxylic functional groups with U and other elements found on the surface of our samples such as K, Fe, or V (Table S2). A peak located between the carboxyl group (289 eV) and carbonyl group (288 eV) was observed at 23.5 ± 0.2 rel% only in the supernatant from the reactor at pH 13 (Figure 1B). A previous study showed that the electrostatic interactions between different chemical moieties cause shifts in the binding energy detected by XPS.[63] For example, the formation of surface complexes (e.g., C−O−M) may cause a shift of the binding energy of carboxylic carbon [C(=O)−OH] to a value lower than the characteristic peak for carboxyl groups alone. Further research is needed to study the mechanism of interaction among specific organic functional groups, U, and other elements occurring in mineralized deposits. Ongoing studies from our research group are assessing the binding of U and organic functional groups in more controlled laboratory environments using XPS, including the possible oxidation of NOM at high pH.

The peak intensity corresponding to phenolic, carbonyl, and carboxylic functional groups as a result of the batch extractions in the reacted solids compared to peaks observed on the unreacted samples decreased except for that of the carbonyl peak after the reaction at pH 13 (Figure S3). Further investigation of the mechanisms and interactions between these functional groups and U in our samples should be pursued.

Effect of pH on U Species. A mixture of U(IV) and U(VI) was detected on the supernatant and reacted solids of all reactors. Fitting of high-resolution XPS U 4f spectra of the reacted solids indicates that the peak intensity corresponding to U(IV) decreased for all reactors relative to those of the unreacted samples, suggesting that U oxidation occurred in the solid sample surface as a result of the reaction conditions tested in our study (Figure S3). The surface concentration of U(VI) in the reacted solids increased by 14.0 rel% at pH 13, 4.4 rel% at pH 7, and 14.6 rel% at pH 2 when compared to that of the unreacted solids.

Analyses of U L_{III} edge XANES spectra also identified a mixture of U(IV) and U(VI) in the reacted solid samples as well as unreacted solids as discussed above (Figure 2). Linear combination fitting of the U L_{III} edge EXAFS spectra detected similar proportions of U(IV) and U(VI) components on reacted solids from batch extraction reactors at pH 7 [46% U(IV) and 54% U(VI)] and pH 2 [49% U(IV) and 51%(VI)] (Table S3). The species of U in the reacted solids likely

DOI: 10.1021/acs.est.9b00407
Environ. Sci. Technol. 2019, 53, 5758−5767

changed as a function of the pH conditions we investigated. Mineral forms of uraninite and coffinite are stable in subsurface environments, while biogenic uraninite and monomeric U(IV) oxidize more readily.[64−66] Previous research has also found U(VI) with reduced U-bearing minerals such as coffinite in the Jackpile Mine.[1,8,45] Similarly, other studies conducted on organic-rich subsurface sediments found U(IV) and U-(VI).[51,67,68]

A mixture of U(IV) and U(VI) was identified using high-resolution XPS U 4f spectra of the supernatant from all batch extractions. The peak intensity corresponding to U(IV) in the supernatant was higher for the reactor at pH 2 and lower for the reactor at pH 13 (Figure 1). While we found U(IV) and U(VI) species in the reacted solids, it is interesting to observe U(IV) in the supernatant from the batch extractions conducted under oxidizing conditions. The U(IV) detected in solution may be U(IV)−NOM colloids, which have been observed in groundwater and wetlands.[69] However, the kinetics of U(IV) species in the supernatant and the mechanisms of formation need to be investigated.

The concentration of U measured in solution in reactors at pH 13 and 2 was similar (34.5 ± 2.78 mg L^{-1} at pH 13 and 40.2 ± 13.49 mg L^{-1} at pH 2), while the concentration of U in solution for the reactor at pH 7 was at least 15-fold lower [1.86 ± 1.28 mg L^{-1} (Figure S4)]. High U concentrations in solution found at pH 2 may be due to the weak adsorption with the solids at this pH. Higher concentrations of U in solution at pH 13 are likely due to the complexation of U with organic functional groups from the NOM and possibly with inorganic ligands, as well. These findings complement the results of XAS analyses that also suggest that the binding between U and NOM decreased in reacted solids. The concentration of U in solution may depend on the co-precipitation of humic substances and the solubility of other U-bearing phases as a function of pH as suggested by other studies.[6,51] Specific mechanisms causing changes in the concentration of soluble U as a function of pH require further investigation in the context of the complex mineralogy of the Jackpile Mine.

■ ENVIRONMENTAL IMPLICATIONS

The main findings of our study indicate that phenolic and carbonyl functional groups are more abundant in the NOM from the Jackpile Mine mineralized deposit samples and show detectable changes on the XPS C 1s spectra after batch extraction at pH 13, 7, and 2. Contrary to what is expected in NOM,[59,60] carboxylic functional groups were the least abundant. Limited changes in the XPS C 1s peaks characteristic of the carboxylic groups were observed as a function of the pH conditions tested in this study. A unique finding of our study is that U(IV) was identified in unreacted solids, exposed to surface oxidizing conditions for several decades, as well as in reacted solids and in the supernatant collected from the batch reaction experiments conducted under oxidizing conditions. In addition to detecting U(IV) in supernatants from batch experiments at pH 13, 7, and 2, we observed noticeable differences in photoelectron peak intensities corresponding to phenolic and carbonyl functional groups in comparison to those for carboxylic functional groups. The organic functional groups in these mineralized deposit samples from the Jackpile Mine could affect the redox, complexation, and precipitation chemistry of U. These chemical reactions could be relevant to the mobilization of the dissolved, colloidal, and particulate forms of U(IV) and U(VI) as shown in other studies.[26,70] For instance, a recent investigation found a high concentration of U(VI) in organic-rich layers as monodentate complexes bound to carboxyl and phosphoryl groups of humic substances above a wetland redox boundary and the complexation of U(IV) by NOM under reducing conditions.[71] Understanding changes in organic functional chemistry at pH 7 and 2 is environmentally relevant due to their influence on chemical reactions that could impact U mobility and transport from the Jackpile Mine to surface waters and plants.[1,36] For example, circumneutral pH conditions are characteristic of surface waters adjacent to the Jackpile Mine, while a lower pH is commonly observed in sites affected by acid mine drainage.[1,45,47] Future research is necessary to identify specific mechanisms through which functional groups from the NOM found in our study control U reactivity at sites with complex mineralogy such as the Jackpile Mine, particularly the influence of NOM on U(IV) stabilization under oxic conditions. This information is essential for the development of risk assessment and remediation strategies at this site and other organic-rich uranium mineral deposits. These findings identify the need for further investigations related to the influence of organic functional groups on heavy metal transport and reactivity.

■ ASSOCIATED CONTENT

Supporting Information

The Supporting Information is available free of charge on the ACS Publications website at DOI: 10.1021/acs.est.9b00407.

Additional materials and methods, Tables S1−S4, and Figures S1−S4 (PDF)

■ AUTHOR INFORMATION

Corresponding Author

*E-mail: jcerrato@unm.edu. Telephone: (001) (505) 277-0870. Fax: (001) (505) 277-1918.

ORCID

Kateryna Artyushkova: 0000-0002-2611-0422
Jorge Gonzalez-Estrella: 0000-0002-4873-0454
José M. Cerrato: 0000-0002-2473-6376

Notes

The authors declare no competing financial interest.

■ ACKNOWLEDGMENTS

The authors acknowledge the existing partnership with the Pueblo of Laguna Environment and Natural Resources Department. The authors also acknowledge the contributions of Dr. Johanna Blake and Dr. Viorel Atudorei for their support and thoughtful comments, which contributed to the significant improvement of this study. Part of this research was carried out at the Stanford Synchrotron Radiation Light Source, a national user facility operated by Stanford University on behalf of the U.S. Department of Energy, OBER. Funding for this research was provided by the National Science Foundation (CAREER Award 1652619) and the National Institute of Environmental Health Sciences Superfund Research Program (Award 1 P42 ES025589).

■ REFERENCES

(1) Blake, J. M.; De Vore, C. L.; Avasarala, S.; Ali, A.-M.; Roldan, C.; Bowers, F.; Spilde, M. N.; Artyushkova, K.; Kirk, M. F.; Peterson, E.; Rodriguez-Freire, L.; Cerrato, J. M. Uranium mobility and

DOI: 10.1021/acs.est.9b00407
Environ. Sci. Technol. 2019, 53, 5758−5767

accumulation along the Rio Paguate, Jackpile Mine in Laguna Pueblo, NM. *Environ. Sci. Process. Impacts.* **2017**, *19* (4), 605−621.
(2) Radionuclides Rule: A quick reference guide. EPA Technical Report 816-F-01-003; Office of Water, U.S. Environmental Protection Agency, 2001.
(3) Hettiarachchi, E.; Paul, S.; Cadol, D.; Frey, B.; Rubasinghege, G. Mineralogy controlled dissolution of uranium from airborne dust in simulated lung fluids (SLFs) and possible health implications. *Environ. Sci. Technol. Lett.* **2019**, *6*, 62.
(4) Jackpile-Paguate uranium mine Laguna Pueblo, NM. U.S. Environmental Protection Agency, 2018 (https://cumulis.epa.gov/supercpad/SiteProfiles/index.cfm?fuseaction=second.cleanup&=0607033).
(5) Spirakis, C. S. The roles of organic matter in the formation of uranium deposits in sedimentary rocks. *Ore Geol. Rev.* **1996**, *11* (1), 53−69.
(6) Cumberland, S. A.; Douglas, G.; Grice, K.; Moreau, J. W. Uranium mobility in organic matter-rich sediments: A review of geological and geochemical processes. *Earth-Sci. Rev.* **2016**, *159*, 160−185.
(7) Birdseye, H. S. Uranium deposits in northern Arizona. In Black Mesa Basin (Northeastern Arizona). In *New Mexico Geological Society 9th Annual Fall Field Conference Guidebook*; Anderson, R. Y., Harshbarger, J. W., Eds.; New Mexico Geological Society: Socorro, NM, 1958; pp 161−163.
(8) Deditius, A. P.; Utsunomiya, S.; Ewing, R. C. The chemical stability of coffinite, $USiO_4 \cdot nH_2O$; 0 < n< 2, associated with organic matter: a case study from Grants uranium region, New Mexico, USA. *Chem. Geol.* **2008**, *251*, 33−49.
(9) Hansley, P. L.; Spirakis, C. S. Organic matter diagenesis as the key to a unifying theory for the genesis of tabular uranium-vanadium deposits in the Morrison Formation, Colorado Plateau. *Econ. Geol. Bull. Soc. Econ. Geol.* **1992**, *87* (2), 352−365.
(10) Leventhal, J. S.; Daws, T. A.; Frye, J. S. Organic geochemical analysis of sedimentary organic matter associated with uranium. *Appl. Geochem.* **1986**, *1* (2), 241−247.
(11) Technical report on technologically enhanced naturally occurring radioactive materials from uranium mining Vol. 1: Mining and reclamation background. EPA Technical Report 402-R-08-005; Office of Radiation and Indoor Air, US Environmental Protection Agency, 2008.
(12) Ellsworth, H. V. Thucholite and uraninite from the Wallingford mine near Buckingham, Quebec. *Am. Mineral.* **1928**, *13* (8), 442−448.
(13) Du, L.; Li, S. C.; Li, X. L.; Wang, P.; Huang, Z. Y.; Tan, Z. Y.; Liu, C. L.; Liao, J. L.; Liu, N. Effect of humic acid on uranium(VI) retention and transport through quartz columns with varying pH and anion type. *J. Environ. Radioact.* **2017**, *177*, 142−150.
(14) Luo, W.; Gu, B. Dissolution and mobilization of uranium in a reduced sediment by natural humic substances under anaerobic conditions. *Environ. Sci. Technol.* **2009**, *43* (1), 152−156.
(15) Sutton, R. S. G.; Sposito, G. Molecular structure in soil humic substances: the new view. *Environ. Sci. Technol.* **2005**, *39*, 9009−9015.
(16) Tinnacher, R. M.; Nico, P. S.; Davis, J. A.; Honeyman, B. D. Effects of fulvic acid on uranium(VI) sorption kinetics. *Environ. Sci. Technol.* **2013**, *47* (12), 6214−6222.
(17) Bordelet, G.; Beaucaire, C.; Phrommavanh, V.; Descostes, M. Chemical reactivity of natural peat towards U and Ra. *Chemosphere* **2018**, *202*, 651−660.
(18) Omar, H. A.; Aziz, M.; Shakir, K. Adsorption of U(VI) from dilute aqueous solutions onto peat moss. *Radiochim. Acta* **2007**, *95* (1), 17−24.
(19) Bone, S. E.; Dynes, J. J.; Cliff, J.; Bargar, J. R. Uranium(IV) adsorption by natural organic matter in anoxic sediments. *Proc. Natl. Acad. Sci. U. S. A.* **2017**, *114* (4), 711.
(20) Daugherty, E. E.; Gilbert, B.; Nico, P. S.; Borch, T. Complexation and redox buffering of iron(II) by dissolved organic matter. *Environ. Sci. Technol.* **2017**, *51* (19), 11096−11104.
(21) Lenhart, J. J.; Cabaniss, S. E.; MacCarthy, P.; Honeyman, B. D. Uranium(VI) complexation with citric, humic and fulvic acids. *Radiochim. Acta* **2000**, *88* (6), 345−353.
(22) von der Heyden, B. P.; Roychoudhury, A. N.; Mtshali, T. N.; Tyliszczak, T.; Myneni, S. C. B. Chemically and geographically distinct solid-phase iron pools in the Southern Ocean. *Science* **2012**, *338* (6111), 1199−1201.
(23) Alessi, D. S.; Lezama-Pacheco, J. S.; Janot, N.; Suvorova, E. I.; Cerrato, J. M.; Giammar, D. E.; Davis, J. A.; Fox, P. M.; Williams, K. H.; Long, P. E.; Handley, K. M.; Bernier-Latmani, R.; Bargar, J. R. Speciation and reactivity of uranium products formed during in situ bioremediation in a shallow alluvial aquifer. *Environ. Sci. Technol.* **2014**, *48* (21), 12842−12850.
(24) Bhattacharyya, A.; Campbell, K. M.; Kelly, S. D.; Roebbert, Y.; Weyer, S.; Bernier-Latmani, R.; Borch, T. Biogenic non-crystalline U(IV) revealed as major component in uranium ore deposits. *Nat. Commun.* **2017**, *8*, 15538.
(25) Bone, S. E.; Cahill, M. R.; Jones, M. E.; Fendorf, S.; Davis, J.; Williams, K. H.; Bargar, J. R. Oxidative uranium release from anoxic sediments under diffusion-limited conditions. *Environ. Sci. Technol.* **2017**, *51* (19), 11039−11047.
(26) Mikutta, C.; Langner, P.; Bargar, J. R.; Kretzschmar, R. Tetra- and hexavalent uranium forms bidentate-mononuclear complexes with particulate organic matter in a naturally uranium-enriched peatland. *Environ. Sci. Technol.* **2016**, *50* (19), 10465−10475.
(27) Bargar, J. R.; Williams, K. H.; Campbell, K. M.; Long, P. E.; Stubbs, J. E.; Suvorova, E. I.; Lezama-Pacheco, J. S.; Alessi, D. S.; Stylo, M.; Webb, S. M.; Davis, J. A.; Giammar, D. E.; Blue, L. Y.; Bernier-Latmani, R. Uranium redox transition pathways in acetate-amended sediments. *Proc. Natl. Acad. Sci. U. S. A.* **2013**, *110* (12), 4506−4511.
(28) Peng, C.; Sundman, A.; Bryce, C.; Catrouillet, C.; Borch, T.; Kappler, A. Oxidation of Fe(II) organic matter complexes in the presence of the mixotrophic nitrate-reducing Fe(II)-oxidizing bacterium acidovorax sp BoFeN1. *Environ. Sci. Technol.* **2018**, *52* (10), 5753−5763.
(29) Scott, D. T.; McKnight, D. M.; Blunt-Harris, E. L.; Kolesar, S. E.; Lovley, D. R. Quinone moieties act as electron acceptors in the reduction of humic substances by humics-reducing microorganisms. *Environ. Sci. Technol.* **1998**, *32* (19), 2984−2989.
(30) Lovley, D. R.; Fraga, J. L.; Blunt-Harris, E. L.; Hayes, L. A.; Phillips, E. J. P.; Coates, J. D. Humic substances as a mediator for microbially catalyzed metal reduction. *Acta Hydrochim. Hydrobiol.* **1998**, *26* (3), 152−157.
(31) Lv, J. T.; Han, R. X.; Huang, Z. Q.; Luo, L.; Cao, D.; Zhang, S. Z. Relationship between molecular components and reducing capacities of humic substances. *ACS Earth Space Chem.* **2018**, *2* (4), 330−339.
(32) Sachs, S.; Geipel, G.; Bernhard, G. Study of the redox stability of uranium(VI) in presence of humic substances. FZKA-7070; Forschungszentrum Rossendorf e.V.: Dresden, Germany, 2005.
(33) Granger, H. C. S. E. S.; Santos, E. S.; Dean, B. G.; Moore, F. B. Sandstone-type uranium deposits at Ambrosia Lake, New Mexico; an interim report. *Econ. Geol. Bull. Soc. Econ. Geol.* **1961**, *56* (7), 1179−1210.
(34) Nash, J. T. Uranium deposits in the Jackpile sandstone, New Mexico. *Econ. Geol. Bull. Soc. Econ. Geol.* **1968**, *63* (7), 737−750.
(35) Adams, S. S.; Curtis, H. S.; Hafen, P. L.; Salek-Nejad, H. Interpretation of postdepositional processes related to the formation and destruction of the Jackpile-Paguate uranium deposit, Northwest New Mexico. *Econ. Geol. Bull. Soc. Econ. Geol.* **1978**, *73* (8), 1635−1654.
(36) El Hayek, E.; Torres, C.; Rodriguez-Freire, L.; Blake, J. M.; De Vore, C. L.; Brearley, A. J.; Spilde, M. N.; Cabaniss, S.; Ali, A.-M. S.; Cerrato, J. M. effect of calcium on the bioavailability of dissolved uranium(vi) in plant roots under circumneutral pH. *Environ. Sci. Technol.* **2018**, *52* (22), 13089−13098.
(37) Yang, Y.; Saiers, J. E.; Barnett, M. O. Impact of interactions between natural organic matter and metal oxides on the desorption

DOI: 10.1021/acs.est.9b00407
Environ. Sci. Technol. 2019, 53, 5758−5767

kinetics of uranium from heterogeneous colloidal suspensions. *Environ. Sci. Technol.* **2013**, *47* (6), 2661−2669.
(38) Yang, Y.; Saiers, J. E.; Xu, N.; Minasian, S. G.; Tyliszczak, T.; Kozimor, S. A.; Shuh, D. K.; Barnett, M. O. Impact of natural organic matter on uranium transport through saturated geologic materials: from molecular to column scale. *Environ. Sci. Technol.* **2012**, *46* (11), 5931−5938.
(39) Bernier-Latmani, R.; Veeramani, H.; Vecchia, E. D.; Junier, P.; Lezama-Pacheco, J. S.; Suvorova, E. I.; Sharp, J. O.; Wigginton, N. S.; Bargar, J. R. Non-uraninite products of microbial U(VI) reduction. *Environ. Sci. Technol.* **2010**, *44* (24), 9456−9462.
(40) Lezama-Pacheco, J. S.; Cerrato, J. M.; Veeramani, H.; Alessi, D. S.; Suvorova, E.; Bernier-Latmani, R.; Giammar, D. E.; Long, P. E.; Williams, K. H.; Bargar, J. R. Long-Term in situ oxidation of biogenic uraninite in an alluvial aquifer: impact of dissolved oxygen and calcium. *Environ. Sci. Technol.* **2015**, *49* (12), 7340−7347.
(41) Massey, M. S.; Lezama-Pacheco, J. S.; Jones, M. E.; Ilton, E. S.; Cerrato, J. M.; Bargar, J. R.; Fendorf, S. Competing retention pathways of uranium upon reaction with Fe(II). *Geochim. Cosmochim. Acta* **2014**, *142*, 166−185.
(42) Ravel, B.; Newville, M. ATHENA, ARTEMIS, HEPHAESTUS: data analysis for X-ray absorption spectroscopy using IFEFFIT. *J. Synchrotron Radiat.* **2005**, *12*, 537−541.
(43) Kuwatsuka, S.; Watanabe, A.; Itoh, K.; Arai, S. Comparison of two methods of preparation of humic and fulvic acids, IHSS method and NAGOYA method. *Soil Sci. Plant Nutr.* **1992**, *38* (1), 23−30.
(44) Santín, C.; Yamashita, Y.; Otero, X. L.; Álvarez, M. Á.; Jaffé, R. Characterizing humic substances from estuarine soils and sediments by excitation-emission matrix spectroscopy and parallel factor analysis. *Biogeochemistry* **2009**, *96* (1), 131−147.
(45) Avasarala, S. Physical and chemical interactions affecting U and V transport from mine wastes. Ph.D. Dissertation, University of New Mexico, Albuquerque, NM, 2018.
(46) Groudev, S.; Georgiev, P.; Spasova, I.; Nicolova, M. Bioremediation of acid mine drainage in a uranium deposit. *Hydrometallurgy* **2008**, *94* (1−4), 93.
(47) Blake, J. M.; Avasarala, S.; Artyushkova, K.; Ali, A.-M. S.; Brearley, A. J.; Shuey, C.; Robinson, W. P.; Nez, C.; Bill, S.; Lewis, J.; Hirani, C.; Pacheco, J. S. L.; Cerrato, J. M. Elevated concentrations of U and co-occurring metals in abandoned mine wastes in a Northeastern Arizona Native American Community. *Environ. Sci. Technol.* **2015**, *49* (14), 8506−8514.
(48) Ohno, T. Fluorescence inner-filtering correction for determining the humification index of dissolved organic matter. *Environ. Sci. Technol.* **2002**, *36* (4), 742−746.
(49) Leventhal, J. S. Organic geochemistry and uranium in Grants mineral belt. *New Mexico Geology and Mineral Technology of the Grants Uranium Region 1979*. Bureau of Mines & Mineral Resources, 1980; Memoir 38, pp 75−85.
(50) Omar, F.; Ruiz, B. M. T.; Cerrato, J. M. Investigation of in situ leach (ISL) mining of uranium in New Mexico and post-mining reclamation. *N. M. Geol.* **2016**, *38*, 77−85.
(51) Cumberland, S. A.; Etschmann, B.; Brugger, J.; Douglas, G.; Evans, K.; Fisher, L.; Kappen, P.; Moreau, J. W. Characterization of uranium redox state in organic-rich Eocene sediments. *Chemosphere* **2018**, *194*, 602−613.
(52) Shoesmith, D. W. Fuel corrosion processes under waste disposal conditions. *J. Nucl. Mater.* **2000**, *282* (1), 1−31.
(53) Fang, Q. L.; Chen, B. L.; Lin, Y. J.; Guan, Y. T. Aromatic and hydrophobic surfaces of wood-derived biochar enhance perchlorate adsorption via hydrogen bonding to oxygen-containing organic groups. *Environ. Sci. Technol.* **2014**, *48* (1), 279−288.
(54) von Gunten, K.; Alam, M. S.; Hubmann, M.; Ok, Y. S.; Konhauser, K. O.; Alessi, D. S. Modified sequential extraction for biochar and petroleum coke: Metal release potential and its environmental implications. *Bioresour. Technol.* **2017**, *236*, 106−110.
(55) Bogusz, A.; Oleszczuk, P.; Dobrowolski, R. Application of laboratory prepared and commercially available biochars to adsorption of cadmium, copper and zinc ions from water. *Bioresour. Technol.* **2015**, *196*, 540−549.
(56) Rahman, A.; El Hayek, E.; Blake, J. M.; Bixby, R. J.; Ali, A. M.; Spilde, M.; Otieno, A. A.; Miltenberger, K.; Ridgeway, C.; Artyushkova, K.; Atudorei, V.; Cerrato, J. M. Metal reactivity in laboratory burned wood from a watershed affected by wildfires. *Environ. Sci. Technol.* **2018**, *52* (15), 8115−8123.
(57) Aiken, G. Fluorescence and Dissolved Organic Matter. In *Aquatic Organic Matter Fluorescence*; Baker, A., Reynolds, D. M., Lead, J., Coble, P. G., Spencer, R. G. M., Eds.; Cambridge University Press: Cambridge, U.K., 2014; pp 35−74.
(58) Zsolnay, A. Chapter 4 - Dissolved Humus in Soil Waters. In *Humic Substances in Terrestrial Ecosystems*; Piccolo, A., Ed.; Elsevier Science B.V.: Amsterdam, 1996; pp 171−223.
(59) Deshmukh, A. P.; Pacheco, C.; Hay, M. B.; Myneni, S. C. B. Structural environments of carboxyl groups in natural organic molecules from terrestrial systems. Part 2:2D NMR spectroscopy. *Geochim. Cosmochim. Acta* **2007**, *71* (14), 3533−3544.
(60) Hay, M. B.; Myneni, S. C. B. Structural environments of carboxyl groups in natural organic molecules from terrestrial systems. Part 1: Infrared spectroscopy. *Geochim. Cosmochim. Acta* **2007**, *71* (14), 3518−3532.
(61) Murphy, R. J.; Lenhart, J. J.; Honeyman, B. D. The sorption of thorium (IV) and uranium (VI) to hematite in the presence of natural organic matter. *Colloids Surf., A* **1999**, *157* (1), 47−62.
(62) Li, D. E.; Kaplan, D. I.; Chang, H. S.; Seaman, J. C.; Jaffe, P. R.; Koster van Groos, P.; Scheckel, K. G.; Segre, C. U.; Chen, N.; Jiang, D. T.; Newville, M.; Lanzirotti, A. Spectroscopic Evidence of Uranium Immobilization in Acidic Wetlands by Natural Organic Matter and Plant Roots. *Environ. Sci. Technol.* **2015**, *49* (5), 2823−2832.
(63) Eby, D. M.; Artyushkova, K.; Paravastu, A. K.; Johnson, G. R. Probing the molecular structure of antimicrobial peptide-mediated silica condensation using X-ray photoelectron spectroscopy. *J. Mater. Chem.* **2012**, *22* (19), 9875−9883.
(64) Alessi, D. S.; Lezama-Pacheco, J. S.; Stubbs, J. E.; Janousch, M.; Bargar, J. R.; Persson, P.; Bernier-Latmani, R. The product of microbial uranium reduction includes multiple species with U(IV)-phosphate coordination. *Geochim. Cosmochim. Acta* **2014**, *131* (C), 115−127.
(65) Cerrato, J. M.; Ashner, M. N.; Alessi, D. S.; Lezama-Pacheco, J. S.; Bernier-Latmani, R.; Bargar, J. R.; Giammar, D. E. Relative reactivity of biogenic and chemogenic uraninite and biogenic noncrystalline U(IV). *Environ. Sci. Technol.* **2013**, *47* (17), 9756−9763.
(66) Guo, X.; Szenknect, S.; Mesbah, A.; Labs, S.; Clavier, N.; Poinssot, C.; Ushakov, S. V.; Curtius, H.; Bosbach, D.; Ewing, R. C.; Burns, P. C.; Dacheux, N.; Navrotsky, A. Thermodynamics of formation of coffinite, $USiO_4$. *Proc. Natl. Acad. Sci. U. S. A.* **2015**, *112* (21), 6551−6555.
(67) Campbell, K.; Kukkadapu, R.; Qafoku, N.; Peacock, A. D.; Lesher, E.; Williams, K. H.; Bargar, J.; Wilkins, M.; Figueroa, L.; Ranville, J.; Davis, J.; Long, P. Geochemical, mineralogical and microbiological characteristics of sediment from a naturally reduced zone in a uranium-contaminated aquifer. *Appl. Geochem.* **2012**, *27*, 1499−1511.
(68) Qafoku, N. P.; Gartman, B. N.; Kukkadapu, R. K.; Arey, B. W.; Williams, K. H.; Mouser, P. J.; Heald, S. M.; Bargar, J. R.; Janot, N.; Yabusaki, S.; Long, P. E. Geochemical and mineralogical investigation of uranium in multi-element contaminated, organic-rich subsurface sediment. *Appl. Geochem.* **2014**, *42*, 77−85.
(69) Wang, Y. H.; Frutschi, M.; Suvorova, E.; Phrommavanh, V.; Descostes, M.; Osman, A. A. A.; Geipel, G.; Bernier-Latmani, R. Mobile uranium(IV)-bearing colloids in a mining-impacted wetland. *Nat. Commun.* **2013**, *4*, 2942.
(70) Mikutta, C.; Kretzschmar, R. Spectroscopic evidence for ternary complex formation between arsenate and ferric iron complexes of humic substances. *Environ. Sci. Technol.* **2011**, *45* (22), 9550−9557.
(71) Stetten, L.; Blanchart, P.; Mangeret, A.; Lefebvre, P.; Le Pape, P.; Brest, J.; Merrot, P.; Julien, A.; Proux, O.; Webb, S. M.; Bargar, J.

DOI: 10.1021/acs.est.9b00407
Environ. Sci. Technol. 2019, 53, 5758−5767

R.; Cazala, C.; Morin, G. Redox fluctuations and organic complexation govern uranium redistribution from U(IV)-phosphate minerals in a mining-polluted wetland soil, Brittany, France. *Environ. Sci. Technol.* **2018**, *52*, 13099.

DOI: 10.1021/acs.est.9b00407
Environ. Sci. Technol. 2019, 53, 5758−5767